Available online at www.sciencedirect.com
SCIENCE DIRECT
Trans. Nonferrous Met. Soc. China 18(2008) 297−302
Transactions of Nonferrous Metals Society of China
www.csu.edu.cn/ysxb/

Effect of Y_2O_3 on microstructure and oxidation of γ-Ni+γ'-Ni_3Al coatings transformed from electrodeposited Ni-Al films at 1 000 ℃

ZHOU Yue-bo(周月波), ZHANG Hai-jun(张海军), WANG Zhen-ting(王振廷)

College of Materials Science and Engineering, Heilongjiang Institute of Science and Technology, Harbin 150027, China

Received 23 May 2007; accepted 14 September 2007

Abstract: The electrodeposited Y_2O_3-dispersed γ-Ni+γ'-Ni_3Al coatings on Ni substrates were developed by the conversion of electrodeposited Ni-Al-Y_2O_3 films with dispersed Al microparticles in Ni matrix into Ni_3Al by vacuum annealing at 800 ℃ for 3 h. For comparison, Y_2O_3-free γ-Ni+γ'-Ni_3Al coatings with a similar Al content were also prepared by vacuum annealing the electrodeposited microparticle-dispersed composite coatings of Ni-Al under the same condition. SEM and TEM characterizations show that the electrodeposited Y_2O_3-dispersed γ+γ' coatings exhibit finer grains, a more homogeneous distribution of γ', and a narrowed γ' phase spacing compared with the electrodeposited Y_2O_3-free γ+γ' coatings. The oxidation at 1 000 ℃ shows that the addition of Y_2O_3 significantly improves the oxidation resistance of the electrodeposited γ+γ'coatings. The effect of Y_2O_3 particles on the microstructure and oxidation behavior of the electrodeposited γ+γ' coatings was discussed in detail.

Key words: electrodeposition; γ-Ni+γ'-Ni_3Al coatings; vacuum annealing; oxidation

1 Introduction

The intermetallic compound γ'-Ni_3Al has attractive applications in the aerospace and power industries as a high-temperature structural material due to its low density, high strength and good oxidation resistance at elevated temperatures[1]. However, the practical use of the intermetallic is still severely restricted by its low-temperature brittleness and poor high-temperature creep resistance. Therefore, applications of the Ni_3Al coatings are a preferred choice for the alloys, especially those with poor oxidation resistance at high temperatures. These coatings are commonly deposited by different techniques of physical vapor deposition(PVD) such as electron beam evaporation[2] and magnetron sputtering [3], or by low pressure plasma spraying[4]. FOSTER et al[5] also suggested that multi-component alloy coatings could be produced by heat treatment of the co-electrodeposited metal matrix/metal or alloy particles composite coating such as Ni-Al[6−9] and Ni-Cr[10−11]. In Refs.[12−14] the microstructure and the oxidation behavior of $\gamma+\gamma'$ or γ' coatings by annealing electrodeposited Ni-Al films have been investigated. IZAKI et al[12] found that such coating with 21%−23% (molar fraction) Al exhibited good oxidation resistance due to the formation of alumina scale. SUSAN et al[13] investigated the inter-diffusion and microstructure of $\gamma+\gamma'$ coating transformed from the electrodeposited Ni-Al films, and found that the $\gamma+\gamma'$ coating with a fine-grain structure exhibited better oxidation resistance than the bulk $\gamma+\gamma'$ alloy[14−15] with a similar Al content, which was also proved by a recent work about the oxidation of $\gamma+\gamma'$ coatings by vacuum annealing the electrodeposited microparticle-dispersed composites of Ni-Al (termed as EMCs Ni-Al) and the electrodeposited nanoparticle- dispersed composites of Ni-Al (termed as ENCs Ni-Al)[16]. In order to improve the cyclic-oxidation resistance of the electrodeposited $\gamma+\gamma'$ or γ' coatings, small amount of CeO_2 was added to the electrodeposited Ni-Al composite coatings[17−18]. Y_2O_3 is another important reactive element oxide to enhance the high temperature performance of alumina-forming alloys and coatings[19]. The objective of this experiment was to gain an understanding of the effect of Y_2O_3 particles on the structure and oxidation of the electro-

Foundation item: Project(06-13) supported by the Scientific Research Startup Foundation of Heilongjiang University of Science and Technology, China
Corresponding author: ZHOU Yue-bo; Tel: +86-451-88036526: E-mail: zhouyuebo760309@163.com; ybzhou@imr.ac.cn

deposited $\gamma+\gamma'$ based coatings with a similar Al content under the same annealing conditions.

2 Experimental

Pure nickel specimens with the size of 15 mm×10 mm×2 mm were cut from a pure electrolytic nickel plate and then were abraded by 800# grit SiC waterproof paper. After being ultrasonically cleaned in acetone, they were electrodeposited with a Ni-Al-Y_2O_3 composite coating (termed as EMCCs Ni-Al-Y_2O_3) from a nickel sulfate bath containing 150 g/L $NiSO_4·7H_2O$, 15 g/L NH_4Cl, 15 g/L H_3BO_3, 0.1 g/L $C_{12}H_{25}NaSO_4$, and certain content of pure Al microparticles with a mean diameter of 2.3 μm and Y_2O_3 microparticles with a average particle size of 2.5 μm. The current density used was 3 A/dm^2, the temperature 35 ℃ and the pH 5.5−6.0. Magnetic stirring was employed to maintain the uniform particles concentration and prevent the sedimentation. In comparison, specimen of Ni-Al composite coating (termed as EMCCs Ni-Al) was also deposited using the same parameters and bath without adding Y_2O_3 microparticles. After being ultrasonically cleaned in distilled water, the EMCCs Ni-Al and EMCCs Ni-Al-Y_2O_3 were annealed in a sealed quartz tube at 800 ℃ for 3 h to form the annealed $\gamma+\gamma'$ coatings with and without Y_2O_3 particles. To exclude the possible oxidation during vacuum annealing, a surface zone with thickness of about 5 μm was ground from the annealed samples using 1000# grit SiC paper. Afterwards, the cross-sectional morphologies and mean Al content of the annealed $\gamma+\gamma'$ coatings were characterized by SEM/EDAX. The Al content of the annealed EMCCs Ni-Al was 7.6% (mass fraction) (termed as A-EMCCs Ni-Al-Y_2O_3), and it was 6.5% for the annealed EMCC Ni-Al-Y_2O_3 (termed as A-EMCCs Ni-Al-Y_2O_3). The crystallinity and microstructure of the annealed $\gamma+\gamma'$ coating with and without Y_2O_3 particles were also investigated by XRD and TEM. Oxidation in air was conducted in a muffle furnace at 1 000 ℃ for 20 h. After certain period of exposure, samples were withdrawn from the furnace for weighting. After 20 h oxidation, surface and cross-sectional morphologies of the scales were investigated by SEM/EDAX.

3 Results

3.1 Coating microstructure

Fig.1 shows the comparison of the XRD patterns of the electrodeposited Ni-Al films before and after annealing at 800 ℃ for 3 h. Clearly, the codeposited Al microparticles were transformed into γ' by the reaction of Al with Ni during annealing, and the position of the Ni peak was shifted to lower angles due to the larger Al atoms incorporating into the Ni lattice.

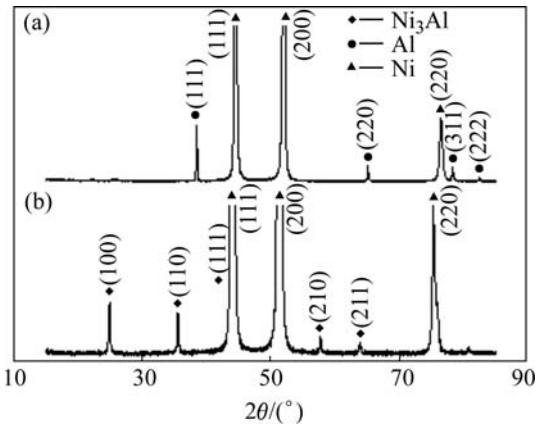

Fig.1 XRD patterns of EMCC Ni-Al (a) and A-EMCC Ni-Al (b)

Fig.2 shows the cross-sectional morphologies of the two annealed coatings with and without Y_2O_3 particles. EDAX analysis indicated that the bright area in the two coatings had 3.0%−4.0%(mass fraction) Al and the gray area with large pores had 9.0%−9.5% Al. From above XED and EDAX analyses, the gray area was γ' phase and the bright area was γ phase. Obviously, the spacing between γ' phases in A-EMCCs Ni-Al-Y_2O_3 was greatly reduced compared with that in A-EMCCs Ni-Al, which suggested that the A-EMCCs Ni-Al-Y_2O_3 had a more uniform distribution of γ' phase. In addition, more and larger pores, mostly formed around γ' phase, were seen in

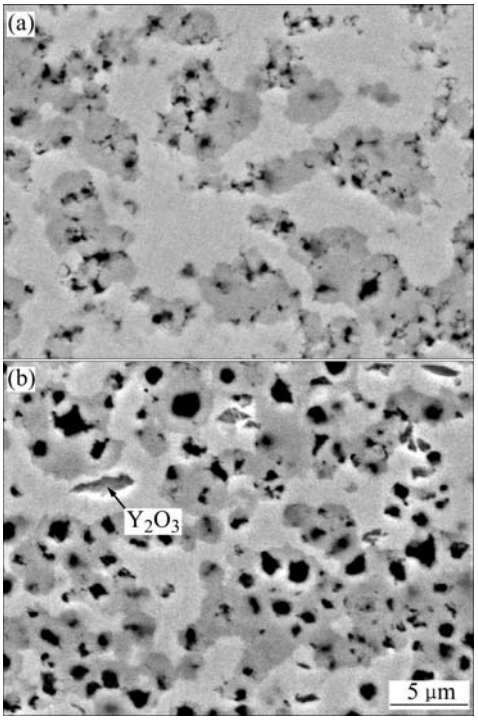

Fig.2 Cross-sectional morphologies of A-EMCCs Ni-Al (a) and A-EMCCs Ni-Al-Y_2O_3 (b)

A-EMCCs Ni-Al-Y_2O_3, as indicated in Fig.2(b). Many investigations[17, 20] showed that pore formation was related to the condensation of excess vacancies, because the phase transformation of Al and Ni to γ' could cause a volume shrinkage. Here, it is noteworthy that the gray blocks in the coatings, indicated by arrows in Fig.2(b), are the dispersed Y_2O_3 particles. They were from the co-deposited Y_2O_3 particles in the composite film. Above results suggest that the Y_2O_3 particles have significantly effect on the interdiffusion, pore formation and reaction of Al with Ni during annealing progress.

The electrodeposited $\gamma+\gamma'$ coatings with and without Y_2O_3 particles were characterized by using TEM, and their images are shown in Fig.3. The average grain size of A-EMCCs Ni-Al was about 1 μm, while the value of A-EMCCs Ni-Al-Y_2O_3 was about 500 nm. Clearly, the A-EMCCs Ni-Al-Y_2O_3 had finer grains than the A-EMCCs Ni-Al due to the addition of Y_2O_3 particles, which suggested that the addition of Y_2O_3 particles retarded the grain growth of the coatings. Fig.3(c) shows a bright-field TEM image of the dispersion bright Y_2O_3 particles in the A-EMCCs Ni-Al-Y_2O_3. It can be seen that near the Y_2O_3 particles, finer grain occurs.

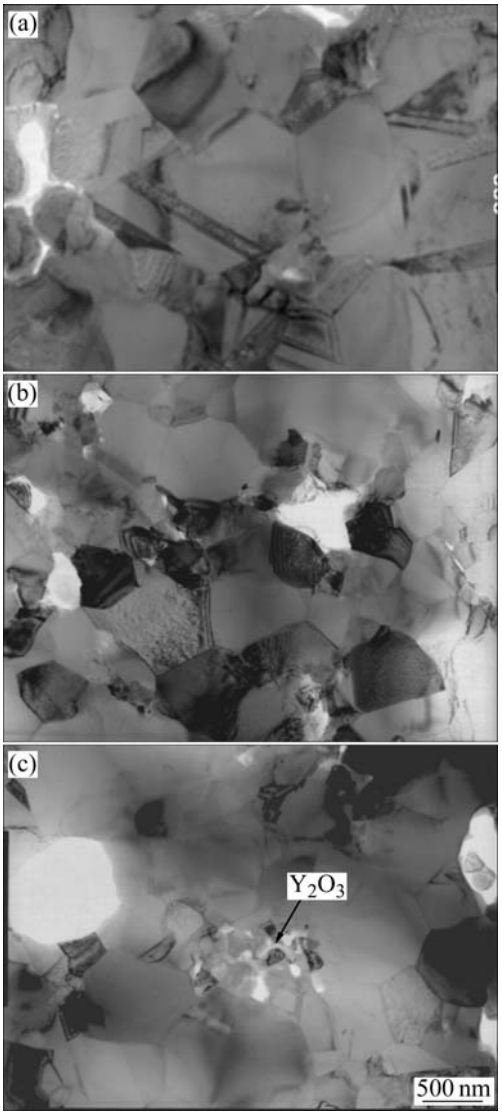

Fig.3 TEM bright-field images of A-EMCCs Ni-Al (a) and A-EMCCs Ni-Al-Y_2O_3 (b, c)

3.2 Oxidation

Oxidation tests were performed in air at 1 000 ℃ for 20 h in a muffle furnace. Fig.4 shows the oxidation kinetics of the two $\gamma+\gamma'$ composites. Both composites obeyed the parabolic rate law. The parabolic rate constant is 1.7×10^{-10} $g^2/(cm^4\cdot s)$ for A-EMCC Ni-7.6Al and 2.3×10^{-11} $g^2/(cm^4\cdot s)$ for A-EMCC Ni-6.5Al-Y_2O_3. Therefore, the $\gamma+\gamma'$ composite from A-EMCC Ni-6.5Al-Y_2O_3 had an oxidation rate over 9 times lower than that from A-EMCC Ni-7.6Al. XRD characterization indicated that oxides formed on the A-EMCC Ni-6.5Al-Y_2O_3 consisted of NiO, $NiAl_2O_4$ and Al_2O_3 with minor NiO, and NiO was the main oxide formed on the A-EMCC Ni-7.6Al. To clarify the difference of the oxidation performance between two coatings, surface and cross-sectional morphologies of the scales were investigated. For the A-EMCC Ni-7.6Al, cubic-shaped NiO grains in a size range of 5−10 μm were formed on the surface, as seen in Fig.5(a). The corresponding cross-sectional scale image is seen in Fig.5(b). The NiO scale was thick and porous, with a dispersion of Al_2O_3 particles in the inner part. And the NiO scale can be divided into two different layers. The outer layer exhibited a porous structure and the inner layer was mixed with minor dispersion of Al_2O_3. No continuous Al_2O_3 scale was observed. Beneath the NiO layer, internal oxidation of aluminum occurred. A similar result was also found for the oxidation of the as-deposited Ni-Al films, which contained Al content below a critical value for the formation of a continuous alumina layer[9]. Surface and corresponding cross-sectional morphologies of scales on the A-EMCC Ni-6.5Al-Y_2O_3 were very

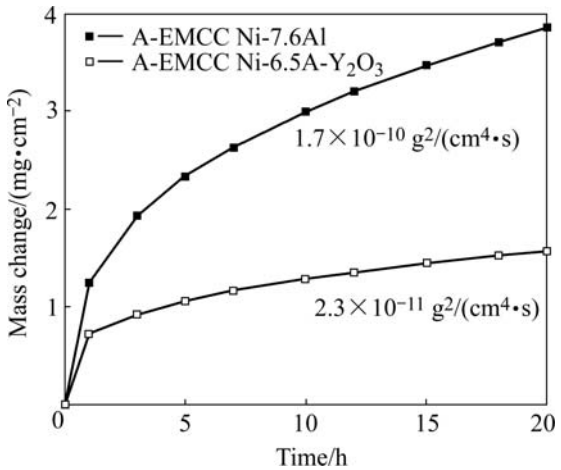

Fig.4 Oxidation kinetics of A-EMCCs Ni-Al with and without Y_2O_3

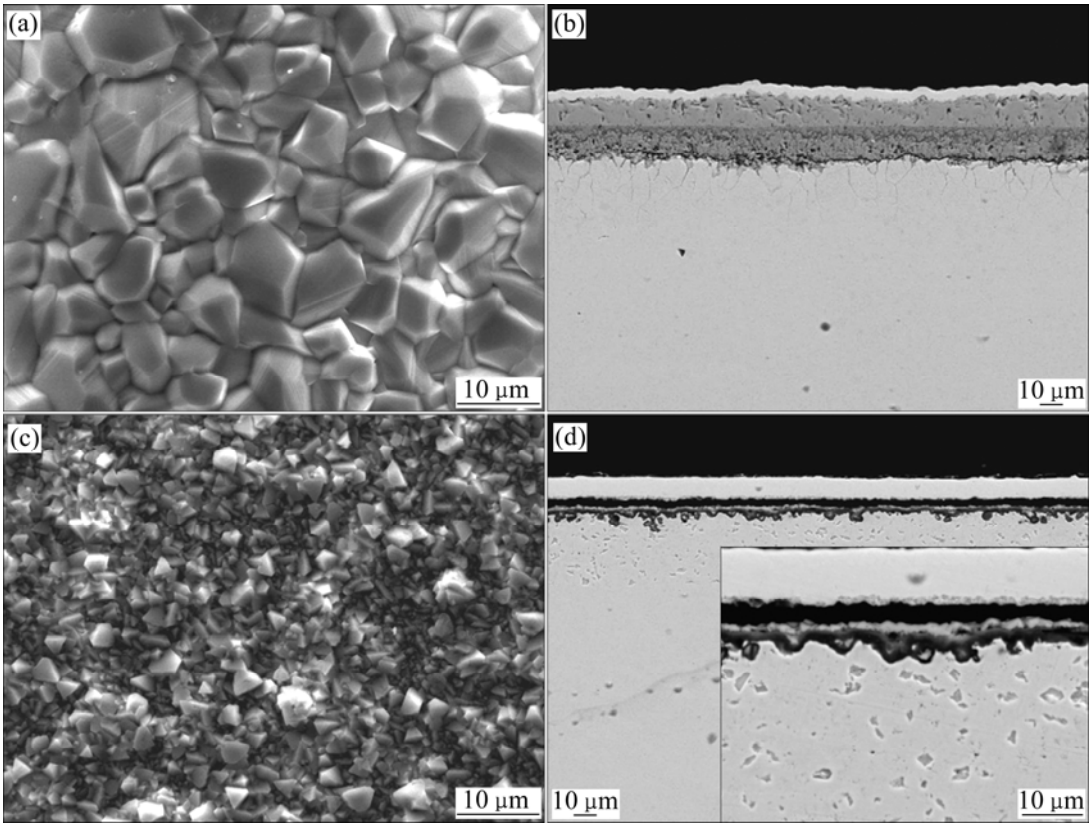

Fig.5 Surface (a, c) and cross-sectional (b, d) morphologies of oxide scales formed on A-EMCC Ni-7.5Al (a, b) and A-EMCC Ni-6.5Al-Y_2O_3 (c, d) after 20 h oxidation in air at 1 000 ℃

different, as seen in Figs.5(c) and (d). The surface oxides were NiO, which had noticeably fine grains in contrast to the oxides on the A-EMCC Ni-7.6Al. As seen from the scale cross-sectional morphology (Fig.5(d) and its inset magnified image), a continuous layer of Al_2O_3 was formed beneath the outer continuous thin NiO layer. A very thin layer of $NiAl_2O_4$ spinel, which appeared darker than outer NiO but lighter than inner Al_2O_3, was sometimes observed between the two layers. The results demonstrated that although the two coatings contained a similar Al content, the A-EMCCs Ni-Al with Y_2O_3 particles exhibited an increasing ability in forming a continuous Al_2O_3 layer.

4 Discussion

Based on this work, the A-EMCC Ni-7.6Al composite was not an alumina former, the same as the work of YANG et al[16]. However, as compared with oxidation of the A-EMCC Ni-7.6Al, the oxidation on the A-EMCC Ni-6.5Al-Y_2O_3 exhibits an extremely low mass gain (Fig.4), as a result of the formation of a continuous alumina scale. From Fig.4, it could be seen that the Y_2O_3-dispered $\gamma+\gamma'$ composites coating exhibits a short-term transient oxidation period and an apparently low scaling rate during the transient period. This is the important reason that the Y_2O_3-dispered coatings oxidize slower than the A-EMCC Ni-7.6Al. The reason is related to the different microstructures of the two coatings, which can be summarized as follows. 1) The A-EMCCs Ni-Al-Y_2O_3 has finer-grain than the A-EMCCs Ni-Al (Fig.3); 2) The spacing between the γ' precipitates is much smaller in the A-EMCCs Ni-Al-Y_2O_3 than in the A-EMCCs Ni-Al (Fig.2). With these characteristics, the A-EMCCs Ni-Al-Y_2O_3 exhibits an increasing ability to grow alumina for the following reasons. At the onset of oxidation, oxides of all elements in the coatings will be formed because the oxygen pressure in the atmosphere is greater than the that of the metal-metal oxide equilibrium. Thus, γ phase of the composite nucleates NiO, and γ' phase nucleates NiO and Al_2O_3[16]. Even though numerous oxide phases are formed during the initial stages of oxidation, there is competition among the elements for oxygen since some of the oxides are more stable than others. As a result of this competition, there is a tendency for the composite eventually to become covered with the most thermodynamically stable oxide according to WAGNER's theory on the transition oxidation[21].

According to WAGNER's theory and PENG's

work[22], in order to form an external oxides scale, the minimum aluminum, N_{Al}, can be estimated by

$$N_{Al}=A\left(\frac{1}{D_L+\frac{2\delta}{d}D_{GB}}\right)^{1/2}$$

where A is a constant, D_L and D_{GB} represent the lattice and grain boundary(GB) diffusivity of aluminum, δ is the GB width and d is the grain size. In metals, D_{GB}/D_L is usually in the range of 10^4−10^6. Thus, N_{Al} will decrease with decreasing d.

For the A-EMCC Ni-7.6Al, the grain size is large, and the Al content is lower than the critical level to form alumina, so a continuous protective Al_2O_3 scales can not be formed by the healing of the Al_2O_3 nuclei through their lateral growth during transient oxidation. The NiO scale grows rapidly and engulfes the Al_2O_3 nuclei at the surface, thus continuous external coarse grains NiO scale without Al_2O_3 oxides are developed. Due to the outward diffusion rate of Ni through Al_2O_3 scale is lower than that through NiO, the presence of Al_2O_3 at the metal/scale interface can have a blocking effect on the outward diffusion of Ni through the NiO scale. In this way, the inward diffusion of oxygen through the outer layer leads to the formation of inner NiO scale with dispersed Al_2O_3 oxides particles[9, 16]. However, for the A-EMCC Ni-6.5Al-Y_2O_3, the grain size is about 500 nm, as seen in Fig.3. If we assume δ=0.5 nm, D_{GB}/D_L=1 000, the critical content of aluminum (N_{Al}) for the A-EMCC Ni-6.5Al-Y_2O_3 will be about 50% of the A-EMCC Ni-7.6Al, which is lower than the critical content to form an alumina oxides scale. Thus, a continuous alumina is formed on the A-EMCC Ni-6.5Al-Y_2O_3, and a low oxidation rate is observed. In addition, a smaller spacing between the γ' precipitates in the A-EMCCs Ni-Al-Y_2O_3 compared with that in the A-EMCC Ni-Al will further reduce the time, which is required for the interconnection of alumina nuclei to form a continuous alumina layer by their lateral growth. Once a continuous Al_2O_3 layer is formed, the growth of NiO is inhibited. The reaction of NiO with Al_2O_3 leads to the formation of $NiAl_2O_4$ spinel in the middle layer. Moreover, the added Y_2O_3 may have a “reactive element effect (REE)”. The selective oxidation of Al is promoted by decreasing the critical content of element for the formation of a continuous protective scale, through providing nucleation sites for Al_2O_3 during initial oxidation and changing the scaling mechanism from dominant outward diffusion in the absence of reactive element into dominant inward oxygen diffusion[20], which needs further investigation.

5 Conclusions

1) The electrodeposited $\gamma+\gamma'$ alloy coatings with and without Y_2O_3 particles were manufactured by vacuum annealing the electrodeposited microparticle-dispersed composite coatings of Ni-Al with and without Y_2O_3 particles at 800 ℃ for 3 h.

2) The oxidation at 1 000 ℃ shows that the Y_2O_3-dispersed $\gamma+\gamma'$ coatings exhibit better oxidation resistance than Y_2O_3-free $\gamma+\gamma'$ coatings at a given Al content due to the formation a continuous protective alumina scale.

3) The effect of Y_2O_3 on the microstructure and oxidation of $\gamma+\gamma'$ coatings transformed from electrodeposited Ni-Al films are summarized as follows. It retards the grain growth of the electrodeposited $\gamma+\gamma'$ coatings during the annealing progress, which significantly enhances Al diffusion to the oxidation front and consequently accelerates the formation of a continuous alumina scale. It also causes a more-homogeneous distribution of γ', and a narrowed γ' phase spacing, which also accelerates the formation of a continuous alumina scale.

References

[1] STOLOFF N S, LIU C T, DEEVI S C. Emerging applications of intermetallics [J]. Intermetallics, 2000, 8: 1313−1320.

[2] NICHOLLS J R, HANCOCK P, AL-YASIRI L H. Optimising oxidation resistance of MCrAl coating systems using vapour phase alloy design [J]. Mater Sci Technol, 1989, 5: 799−805.

[3] WANG F. Oxidation resistance of sputtered Ni_3(AlCr) nanocrystalline coating [J]. Oxidation of Metals, 1997, 47: 247−258.

[4] KANG Z X, NAKATA K, LI Y Y. Hard thick-film and wear resistance of Al-50Si-10M ternary alloys on A6063 aluminum alloy coated low pressure plasma spraying [J]. Surf Coat Tech, 2007, 201: 4999−5002.

[5] FOSTER J, CAMERON B P, CAREW J A. The production of multi-component alloy coatings by particles codeposition [J]. Trans Inst Met Finish, 1985, 63: 115−119.

[6] SUSAN D F, MARDER A R, BARMAK K. Electrodeposited Ni-Al particle composite coatings [J]. Thin Solid Films, 1997, 307: 133−139.

[7] LIU H F, CHEN W X. Electrodeposited Ni-Al composite coatings with high Al content by sediment co-deposition [J]. Surf Coat Tech, 2005, 191: 341−350.

[8] ZHOU Y, PENG X, WANG F. Oxidation of a novel electrodeposited Ni-Al nanocomposite film at 1 050 ℃ [J]. Scripta Mater, 2004, 50: 1429−1433.

[9] ZHOU Y, PENG X, WANG F. Size effect of Al particles on the oxidation of electrodeposited Ni-Al composite coatings [J]. Oxidation of Metal, 2005, 64: 169−183.

[10] BAZARD R, BODEN P J. Nickel-chromium alloys by codeposition (part Ⅱ): Diffusion heat treatment of codeposited composite [J]. Trans Inst Met Finish, 1972, 50: 207−210.

[11] ZHANG Y, PENG X, WANG F. Development and oxidation at 800 ℃ of a novel electrodeposited Ni-Cr nanocomposite film [J].

Materials Letters, 2004, 58: 1134−1138.

[12] IZAKI M, FUKUSUMI M, ENOMOTO H, OMI T, NAKAYAMA Y. High-temperature oxidation resistance of Ni-Al Alloy films, prepared by heating electrodeposited composite [J]. J Japan Inst Met, 1993, 57: 182−189.

[13] SUSAN D F, MISIOLEK W Z, MARDER A R. Reaction synthesis of Ni-Al-based particle composite coatings [J]. Metall Mater Trans, 2001, 32A: 379−390.

[14] SUSAN D F, MARDER A R. Oxidation of Ni-Al-based electrodeposited composite coatings Ⅰ: Oxidation kinetics and morphology at 800 ℃ [J]. Oxid Met, 2002, 57: 131−157.

[15] SUSAN D F, MARDER A R. Oxidation of Ni-Al-based electrodeposited composite coatings Ⅱ: Oxidation kinetics and morphology at 1 000 ℃ [J]. Oxid Met, 2002, 57: 159−180.

[16] YANG X, PENG X, WANG F. Size effect of Al particles on the structure and oxidation of Ni/Ni_3Al composites transformed from electrodeposited Ni-Al films [J]. Script Mater, 2007, 56: 509−512.

[17] ZHOU Y, PENG X, WANG F. Cyclic oxidation of alumina-forming Ni-Al nanocomposites with and without CeO_2 addition [J]. Script Mater, 2006, 55: 1039−1042.

[18] LIU H F, CHEN W X. Cyclic-oxidation behavior of electrodeposited Ni_3Al-CeO_2 based coatings at 850 ℃ [J]. Oxidation of Metals, 2005, 64(5/6): 331−354.

[19] UL-HAMID A. TEM study of the effect of Y on the scale microstructures of Cr_2O_3- and Al_2O_3-forming alloys [J]. Oxidation of Metals, 2002, 58(1/2): 23−40.

[20] MOON D P. Role of reactive elements in alloy protection [J]. Mater Sci Technol, 1989, 5: 754−763.

[21] WAGNER C. Type of reaction on the oxidation of alloys [J]. Z Elektroch, 1959, 63: 772−782.

[22] PENG X, WANG F. Morphologic investigation and growth of the alumina scale on magnetron-sputtered CoCrAl NCs with and without yttrium [J]. Corrosion Science, 2003, 45(10): 2293−2306.

(Edited by YANG Bing)